RASĀYAN *J. Chem.*
Vol. 18 | No. 1 |538-545| January - March | 2025
ISSN: 0974-1496 | e-ISSN: 0976-0083 | CODEN: RJCABP
http://www.rasayanjournal.com
http://www.rasayanjournal.co.in

BIOSYNTHESIS OF SILVER NANOPARTICLES USING A MIXED AQUEOUS EXTRACT OF FICUS RELIGIOSA BARK, LEAF, AND ROOT: FREE RADICAL INTERACTIONS AND ANTIBACTERIAL EVALUATION

Vivek Yadav✉, Surendra Singh Tak, Himmat Singh and Kailash Daga
Department of Chemistry, Jai Narain Vyas University Jodhpur, Rajasthan, 342011
✉Corresponding author: vivekyvivek@yahoo.co.in

ABSTRACT

Silver nanoparticles have attracted a lot of interest for their many uses, especially in the pharmaceutical industry, because of their remarkable pharmacological characteristics. Among the several synthesis techniques, those that use plant-based extracts, particularly from medicinal herbs—have grown in popularity. Ficus religiosa, also known as the peepal tree and a member of the Moraceae family has been used traditionally for many years because of its anti-cancer, anti-ulcer, antibacterial, and anti-diabetic qualities. In this study, a mixed aqueous extract of Ficus religiosa's bark, leaf, and root was used to reduce silver ions and create AgNPs. A variety of analytical methods, such as FTIR, TEM, XRD, and UV, were then used to characterize the nanoparticles. A distinctive absorption peak at 424 nm was found by UV spectroscopy examination, suggesting the creation of AgNPs. The crystalline character of the produced AgNPs was validated by XRD examination. The existence of functional groups such as alcohols, alkenes, alkynes, and alkyl halides was shown by FTIR spectra, and these groups most likely aid in the stability and capping of the nanoparticles. The majority of the nanoparticles were spherical, with an average size of 50-70nm, according to TEM imaging. The produced AgNPs' antibacterial activity was assessed against a variety of bacterial species, such as *Pseudomonas aeruginosa, Bacillus subtills, Escherichia coli, and Staphylococcus aureus*. The inhibitory zones that developed around the nanoparticles demonstrated the AgNPs' strong antibacterial activity. Additionally, the 2,2-diphenylpicrylhydrazyl (DPPH) free radical scavenging experiment was used to evaluate the produced nanoparticles' antioxidant capability. The reduction in absorbance of the DPPH solution showed that the AgNPs exhibited significant antioxidant activity, successfully trapping up to 75% of free radicals.

Keywords: Silver Nanoparticles, Antibacterial, Antioxidant, TEM, XRD

RASĀYAN *J. Chem.*, Vol. 18, No.1, 2025

INTRODUCTION

Because of its many uses, such as surface-enhanced Raman scattering, electrical conductivity, antibacterial qualities, magnetic and optical polarity, and catalytic activity, the creation of nanoparticles (NPs) has become a key field in nanotechnology.[1–5] Silver nanoparticles (AgNPs) are often produced using a variety of methods, including photoreduction, thermal breakdown in organic solvents, and chemical reduction of silver ions in aqueous solutions.[6–9] These traditional approaches, however, can include costly processes and the use of hazardous chemicals, which present serious concerns to public health and safety. On the other hand, the biosynthesis of AgNPs using plant extracts provides a quick, affordable, and environmentally beneficial alternative. This one-step process is safe for possible therapeutic uses in humans and is not harmful to the environment.[10–11] The biogenesis of AgNPs from plant extracts has been the subject of several investigations; in India, Azadirachta indica, Ficus religiosa, Pelargonium graveolens, Medicago sativa, and Emblica officinalis are a few examples. The holy fig, or Ficus religiosa, has long been renowned for its therapeutic qualities, especially in South Asia. A variety of illnesses, including bacterial and protozoal infections, viral disorders, diarrhea, gonorrhea, cancer, inflammation, asthma, ulcers, and other skin issues, have historically been treated using the bark, leaves, and fruits of this tree.[12–15] Using a combined aqueous extract of Ficus religiosa's bark, leaves, and roots—which blends extracts from many plant parts—we sought to create AgNPs in this investigation. Although comparable studies have employed separate extracts, this study is unusual since it uses a combined extract, which also enables a comparison of the size and therapeutic effectiveness of AgNPs made from various plant sections. A range of metabolites, such as proteins, amino acids, carbohydrates, flavonoids, terpenoids, saponins, nitrogenous

http://doi.org/10.31788/RJC.2025.1819198

bases, and reducing sugars are involved in the reduction and stabilization of silver ions into nanoparticles and drive the biosynthesis of AgNPs in this context.[16–19] The size, shape, and general efficacy of the produced AgNPs—which may have a variety of uses in the biological and technical domains—are all influenced by these metabolites, which are essential to the distinct potential of each plant extract. Furthermore, since plant extracts include a diverse range of bioactive substances, including proteins, reducing sugars, phenolic compounds, flavonoids, and terpenoids, they are acknowledged as very efficient reducing and stabilizing agents in the creation of nanoparticles. The produced AgNPs were tested in this work for their antibacterial efficacy against strains of bacteria that were the nanoparticles were tested against Gram-positive bacteria (*Bacillus subtilis and Staphylococcus aureus*) and Gram-negative bacteria *(Escherichia coli and Pseudomonas aeruginosa*). Additionally, their antioxidant capacity was assessed, highlighting their potential for medicinal applications. The biosynthesized AgNPs' therapeutic potential was confirmed by both assessments, which showed significant biological activity.

EXPERIMENTAL

Every chemical and reagent utilized in this investigation was of analytical quality and didn't need any further purification. Sigma-Aldrich provided the 99% silver nitrate and 99% DPPH. Before being utilized, the glassware used in the experiment was dried in a hot air oven after being properly cleaned with double-distilled water. During the whole experiment, distilled water was used. The Mumbai, India-based HI Medium Laboratories Pvt. Ltd. provided the microbiological medium needed for the investigation. Centrifugation, drying, powdering, calcination, extraction, reagent synthesis, and the creation of the aqueous reagent solution were among the procedures used to create AgNPs.

Collection of Plant Material and Extraction Process

Ficus religiosa (FR) leaves, bark, and roots were gathered from their natural environments, carefully washed with distilled water, and then broken into little pieces for further processing. To get rid of any surface dirt, the materials were first cleaned with tap water. This was followed by several rinses with distilled water. After that, the samples were left to air dry for two to four days in the shade. The plant parts were dried, then powdered into a fine powder, and kept in airtight containers. A 1:10 (powder/solvent) ratio was used to combine 100 milliliters of methanol with around 10 grams of the powdered material. The resultant mixture was heated to between 35°C and 50°C in a shaker incubator. Following a 12-hour incubation period, the extract was collected and refrigerated for further use in the experiments.

Preparation of 1 mM Silver Nitrate Solution

3.4 grams of silver nitrate ($AgNO_3$) were dissolved in 20 milliliters of double-distilled water to create a 1M stock solution. One milliliter of the 1 M stock solution was diluted with 99 milliliters of double-distilled water to create a 100-milliliter solution. After that, this 1 mM solution was put away for use in the research later on.

Biosynthesis of AgNPs

The 1 mM silver nitrate solution served as the starting point for the creation of silver nanoparticles (AgNPs). At a temperature between 50°C and 60°C, 100 ml of the 1 mM $AgNO_3$ solution was added dropwise to a 10 ml aliquot of the combined extract in a conical flask while being continuously stirred. The combination was left to incubate at room temperature while the color change was regularly observed. The effective synthesis of AgNPs was indicated by the blended extract's first color shift from light green to faint brown and then from faint brown to dark brown. To aid in the creation of nanoparticles, various amounts of the combined leaf, bark, and root extract as well as varied concentrations of $AgNO_3$ Figures were made in different test tubes and incubated for a whole day.

Characterization

An infrared spectrometer (FTIR) from Perkin Elmer was employed to record the infrared spectra. Powder X-ray diffraction (PXRD) measurements were performed using a Bruker D8 Advance X-ray diffractometer equipped with a sealed tube producing X-rays at a wavelength of 0.154 nm (Cu K-alpha). Detection of the X-rays was carried out using the Bruker Lynx Eye detector, a high-speed silicon strip-based system. The PXRD measurements were conducted under operating conditions of 40 kV and 40 mA. The surface

morphology of the synthesized nanoparticles at various resolutions was examined using a JEOL scanning electron microscope (SEM) from Japan. A transmission electron microscope (TEM, JEOL JEM 2100F) operating at an accelerating voltage of 120 kV was used to further analyze the nanoparticles' size. A drop of the dispersed nanoparticles was applied on a 3 mm copper grid covered with a carbon sheet to produce samples for TEM analysis. A negative stain of ammonium molybdate (pH 7.5) that had been filtered via a 0.45 µm filter was applied to the grid. Before imaging, the grid was let to air dry at room temperature after any excess stain on its borders was removed using filter paper.

DPPH Interaction Analysis (Antioxidant Activity)

The capacity of stable DPPH to scavenge free radicals was used to measure the antioxidant activity (AA).[20-21] AgNPs were sonicated in methanol to create solutions with different concentrations (0.01%, 0.03%, 0.05%, 0.07%, and 0.09%). In the same solvent, a stock solution of DPPH (0.002%) was also made. Two milliliters of the DPPH solution and two milliliters of each AgNP solution were combined, and the mixture was agitated briskly to guarantee homogeneity before the antioxidant activity was assessed. After that, the sample solutions were left to incubate for one and a half hours in the dark. First, methanol blank spectra were acquired. The absorption spectra were then obtained by spectrophotometric titration using different amounts of AgNPs. A Spectro 2060 Plus model UV/Vis spectrophotometer was used to measure the absorbance of the DPPH solution at 517 nm since this is the wavelength at which DPPH shows its typical maximum absorption. The antioxidant activity was determined by measuring the absorbance at 517 nm; a greater absorbance decrease suggested that the AgNPs had a more remarkable capacity to scavenge free radicals.

Antimicrobial Analysis

The disc diffusion technique on Mueller Hinton agar was used to assess the produced AgNPs' antibacterial activity.[22,23] To evaluate the antimicrobial qualities of the AgNPs, the study concentrated on two Gram-negative bacterial species (*Escherichia coli* MTCC448/ATCC9637 and *Pseudomonas aeruginosa* MTCC1934/ATCC10415) and two Gram-positive bacterial species (*Bacillus subtilis* MTCC121/ATCC6051 and *Staphylococcus aureus* MTCC1430/ATCC12600). Mueller Hinton agar (38 g/L) autoclaved for sterilization was employed as the culture medium for the antibacterial test. To culture the bacteria, six distinct Petri plates were made and freshly dried in an oven. Using sterile cotton swabs, a bacterial suspension was applied to the agar surface at a standard concentration of 1000 CFU/mL for each species. The infected agar plates were subsequently covered with sterile autoclaved filter paper discs that had been impregnated with different quantities (25, 50, 75, and 100 mg/mL) of the AgNPs made using the leaf extract. To evaluate the antibacterial efficacy of the AgNPs, the inhibition zones around each disc were measured in millimeters using a ruler after the plates were incubated for 48 hours at 37°C. The antibacterial efficacy of the produced nanoparticles against the tested bacterial strains was shown by clear inhibition zones.

RESULTS AND DISCUSSION

Extraction and Synthesis of AgNPs

Methanol and powdered Ficus religiosa (FR) leaves, bark, and root were combined in a 1:10 ratio (1 g of plant material in 10 ml of methanol). After a 12-hour incubation period in a shaker, the extract was kept in a refrigerator at 4°C (Fig.-1). A silver nitrate solution was mixed with the extract, and the color shift was observed for a whole day. The solution changed from light yellow to dark brown throughout incubation; this color shift is ascribed to the surface plasmon resonance (SPR) vibration, which indicates that the nanoparticles (NPs) were successfully synthesized.

Characterization of Synthesized AgNPs

UV- Visible and FTIR Spectroscopy

4 ml of the combined Ficus religiosa (FR) extract was mixed with different concentrations of silver nitrate ($AgNO_3$) in amounts of 10, 20, 30, 40, 50, and 60 µl. The mixture was then adjusted with 6 ml of double-distilled water. UV-visible spectroscopy was first used to identify and characterize the produced silver nanoparticles (AgNPs). At a concentration of 40 µl, the greatest amount of AgNPs was produced. The production of AgNPs decreased along with the blended extract's content. Surface plasmon resonance (SPR)

vibrations caused the extract's color to shift from green to brown, signifying the creation of nanoparticles. The existence of synthetic silver nanoparticles was verified by the absorption peak at 424 nm in the UV-visible spectra, which were collected from 300 nm to 700 nm (Fig.-2).

Fig.-1: Mix Extract of Ficus Religiosa Leaves + Bark + Root

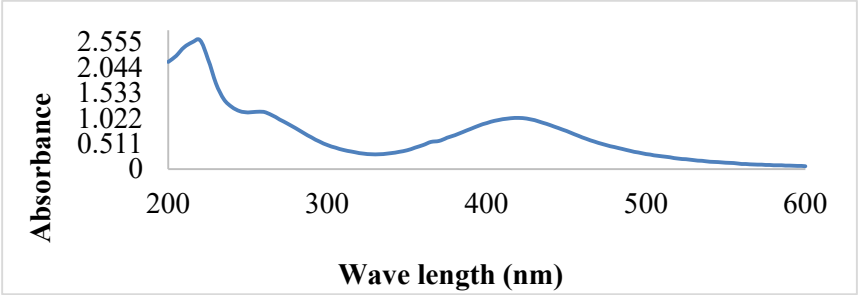

Fig.-2: UV-Visible Spectra of Synthesized AgNPs

As the extract concentration rose, a progressive drop in absorbance and a change in the peak wavelength from 430 nm to lower values were seen. Changes in particle size and shape that impact the surface plasmon resonance may be the cause of this shift. According to earlier research, AgNPs have comparable absorption maxima between 400 and 450 nm.[25] To determine which functional groups in the biomolecules were in charge of reducing Ag^{+} and stabilizing the AgNPs, Fourier-transform infrared (FTIR) analysis was performed. To determine these functional groups, the observed peaks at 3325.45 cm^{-1}, 2114.88 cm^{-1}, 1637.47 cm^{-1}, 584.34 cm^{-1}, and 523.76 cm^{-1} (Fig.-3) were compared with standard values. The existence of an alcohol group is shown by the peak at 3325 cm^{-1}, which corresponds to O-H stretching. An alkyne group is present because the peak at 2114 cm^{-1} corresponds to C≡C stretching. The existence of an alkene group is shown by the peak at 1637 cm^{-1}, which corresponds to C=C stretching. The presence of an alkyl halide group is shown by the peaks at 584 cm^{-1} and 523 cm^{-1}, which correspond to C-Br stretching.[26]

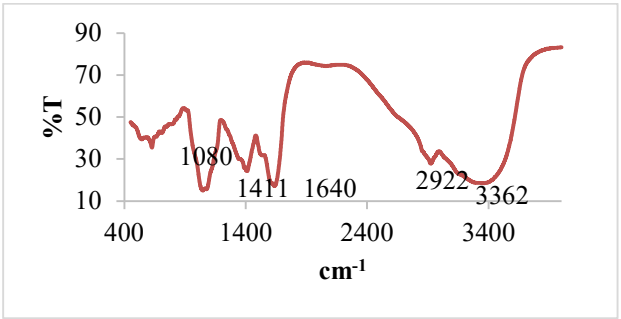

Fig.-3: FTIR Analysis of Synthesized AgNPs

X-ray diffraction (XRD) examination verified that the produced AgNPs were crystalline. Figure-4 displays the XRD pattern, which was captured between 10° and 100°. There were many different Bragg reflections

at 27°, 33°, 46°, 55°, 57°, and 77°. The 111, 200, and 311 planes of the face-centered cubic (FCC) structure of silver nanoparticles are represented by the 33°, 46°, and 77° peaks. These findings are in line with a number of investigations that have shown the cubic structure of AgNPs produced physiologically.[27]

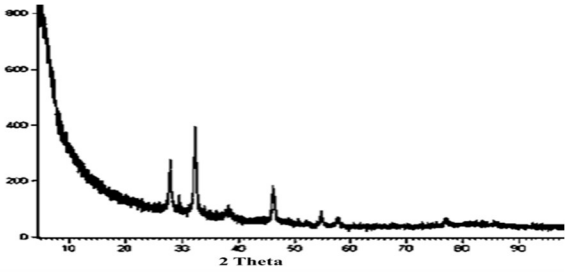

Fig.-4: Powder XRD Pattern of Synthesized AgNPs

Scherrer's equation was used to calculate the NPs' crystalline size, as shown in Figure above.[28]

$$D = \frac{0.9\lambda}{\beta \cos \theta}$$

The Scherrer equation was used in this investigation to ascertain the crystalline size of the produced silver nanoparticles (AgNPs): where *D* is the crystalline size, *λ* is the wavelength of the incoming X-ray (0.154 nm), *β* is the full-width at half maximum (FWHM), and *θ* is the angle of diffraction in radians. It was discovered that the average crystalline size was between 50 and 70 nm. The shape of the generated AgNPs was revealed by Scanning Electron Microscopy (SEM) examination (Fig.-5), which showed that the particles were mostly spherical. The size of the AgNPs, which varied from 68 nm to 89 nm, was further validated by Transmission Electron Microscopy (TEM) examination, as seen in Fig.-5. These findings further supported the effective production of the nanoparticles by being in accordance with their crystalline nature and form.

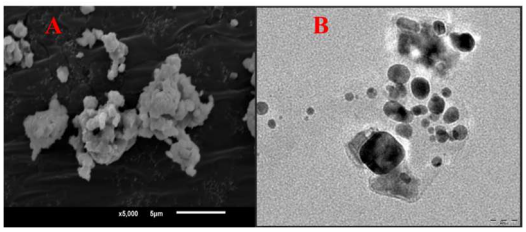

Fig.-5: SEM (A) and TEM (B) Analysis of Biosynthesized AgNPs

Antimicrobial Investigation

Using the Müller-Hinton agar disk diffusion method, the antimicrobial activity (AA) of the synthesized AgNPs was assessed against two Gram-positive bacterial species, *Bacillus subtilis* (MTCC121/ATCC6051) and *Staphylococcus aureus* (MTCC1430/ATCC12600), as well as two Gram-negative bacterial species, *Escherichia* coli (MTCC448/ATCC9637) and *Pseudomona aeruginosa* (MTCC1934/ATCC10415). As positive controls, cefoxitin (FOX) and tetracycline (TE) at dosages of 10 µg, 30 µg, and 30 µg per disc showed suppression of bacterial growth. As a negative control, the extract from Ficus religiosa (FR) had no antibacterial activity (Fig.-6).

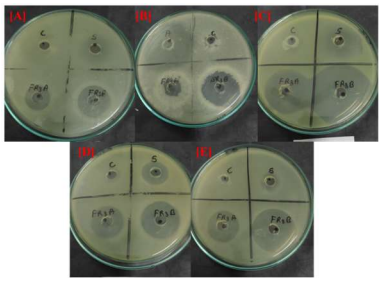

Fig.-6: Antimicrobial Analysis of Synthesized AgNPs where A, B, C, D, and E Stand for Cefoxitin, Tetracycline, AgNPs (20 mg/mL), AgNPs (40 mg/mL) and AgNPs (60 mg/mL)

The efficacy of AgNPs was compared with the positive and negative controls, and the findings were evaluated according to the existence or lack of inhibitory zones around the discs.

Table-1: Zone Inhibition of FeO_NPs on Bacterial Culture

No.	Test material	Zone of inhibition (Diameter in mm)			
		Escherichia coli MTCC448/ ATCC9637	*Pseudomonas aeruginosa* MTCC1934/ ATCC10415	*Staphylococcus aureus* MTCC1430/ ATCC12600	*Bacillus subtilis* MTCC121/AT CC6051
1	Cefoxitin (FOX) (30 µg/disc)	22 mm	17 mm	11 mm	7 mm
2	Tetracycline (TE) (30 µg/disc)	27 mm	22 mm	10 mm	9 mm
3	AgNPs (20 mg/mL)	12 mm	5 mm	NA	NA
4	AgNPs (40 mg/mL)	16 mm	7 mm	NA	NA
5	AgNPs (60 mg/mL)	21 mm	11 mm	5 mm	7 mm

The zone of inhibition (ZOI) for AgNPs against the four pathogens in comparison to conventional antibiotics is shown in Table-1. The findings showed that the inhibition zones of Gram-negative bacteria were greater than those of Gram-positive bacteria. Their cell walls' structural features are probably the cause of this discrepancy. Gram-negative bacteria have an outer membrane made of phospholipids and lipopolysaccharides, whereas Gram-positive bacteria have thick peptidoglycan layers with teichoic acids. Gram-negative bacteria have a higher ZOI than Gram-positive bacteria because their outer membranes are negatively charged, which may allow for more efficient interactions with the positively charged AgNPs. Gram-negative bacteria often exhibit bigger inhibitory zones than Gram-positive bacteria, according to earlier research.[3,30] This may be explained by the positively charged AgNPs' increased capacity to pierce the bacterial surface due to their electrostatic attraction to the negatively charged elements of the Gram-negative bacterial cell wall. AgNPs' primary mechanism of antibacterial activity is believed to be their interaction with bacterial cells' thiol groups (-SH), which results in structural changes that prevent DNA replication and protein synthesis.[33–35] Furthermore, membrane proteins may become unstable as a consequence of the electrostatic interaction between the negatively charged bacterial surfaces and the positively charged AgNPs, disrupting the cell membrane and eventually leading to cell death.[36] In order to further aid in the deactivation of bacteria, AgNPs may also be adsorbed onto their surfaces and engage in photocatalytic oxidation processes.[32]

Antioxidant Activity

Due to a reduction in DPPH's absorbance, the AA (%) of AgNPs was computed as follows:

$$Scavenging\ Activity\ \% = \frac{A_o - A_s}{A_o}$$

Where As represents the absorbance of DPPH• in the presence of AgNPs and A0 represents the absorbance of DPPH• in the absence of a pharmacological molecule. Table-3 and Fig.-7 provide a summary of the antioxidant activity computations, showing the mean ± standard deviation (SD) of three measurements.

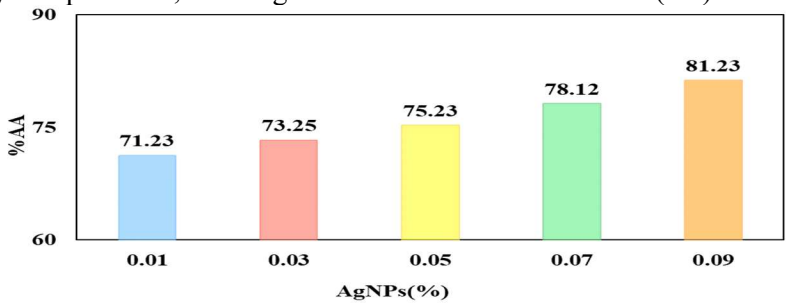

Fig.-7: Antioxidant Activity Analysis of Synthesized AgNPs

With an antioxidant activity of up to 78%, the produced AgNPs showed notable radical trapping activity. The observed color shift, where the violet hue of the DPPH solution becomes yellow when AgNPs are added, makes this high activity level clear. The percentage of antioxidant activity (AA) rose in tandem with the AgNPs concentration, indicating that a larger concentration of AgNPs offered more particles to bind with and trap the DPPH molecules. The production of Ag+ ions from AgNPs, which interact with the free electrons in the DPPH molecule, maybe the mechanism behind this radical entrapment. Because of this interaction, DPPH radicals are reduced, which adds to the AgNPs' apparent antioxidant efficacy.

CONCLUSION

This work used an aqueous extract of Ficus religiosa, a plant with important medicinal effects, to effectively show the manufacture of silver nanoparticles (AgNPs). The effective synthesis, crystalline nature, and spherical shape of the produced AgNPs were validated by characterization utilizing Fourier-transform infrared spectroscopy (FTIR), transmission electron microscopy (TEM), X-ray diffraction (XRD), and UV-visible spectroscopy. The AgNPs show significant antibacterial activity, effectively inhibiting a variety of bacterial pathogens, such as Pseudomonas aeruginosa, Bacillus subtilis, Escherichia coli, and Staphylococcus aureus. Additionally, the AgNPs' significant radical scavenging capabilities in the DPPH experiment indicated that they exhibited substantial antioxidant activity. These results highlight the potential of AgNPs produced from Ficus religiosa as viable candidates for medical applications, especially in the development of new antioxidant and antibacterial therapeutic agents.

ACKNOWLEDGMENTS

The authors are thankful to Jai Narain Vyas University Jodhpur, Rajasthan for providing infrastructure and facilities.

CONFLICT OF INTERESTS

The authors declare that there is no conflict of interest.

AUTHOR CONTRIBUTIONS

All the authors contributed significantly to this manuscript, participated in reviewing/editing, and approved the final draft for publication. The research profile of the authors can be verified from their ORCID ids, given below:

Vivek Yadav http://orchid.org/ 0009-0003-2013-2246
Kailash Daga http://orchid.org/ 0009-0006-9062-7879
Surendra Singh Tak https://orcid.org/0009-0002-3525-7896
Himmat Singh https://orcid.org/0009-0005-6148-5990

REFERENCES

1. P. Raveendran, J. Fu, S. L. Wallen, *Green Chemistry,* **8**, 34(2006), https://doi.org/10.1039/B512540E
2. Sriramulu Arava, L. Valluru, *International Journal of Pharmacy and Biological Sciences,* **9(2)**, 571(2019), https://doi.org/10.21276/ijpbs.2019.9.2.71
3. L. T. Chang, C. C. Yen, *Journal of Appllied Polymer Science,* **55(2),** 371(1995), https://doi.org/10.1002/app.1995.070550219
4. A. R. Sharverdi, S. Mianaeian, H. R. Shahverdi, H. Jamalifar, A.A Nohi, *Process Biochemistry*, **42(5),** 919(2007), https://doi.org/10.1016/j.procbio.2007.02.005
5. P. Matejka, B. Vlckova, J. Vohlidal, P. Pancoska V. Baumruk, *The Journal of Physical Chemistry*, **96(3),** 1361(1992), https://doi.org/10.1021/j100182a063
6. L. M. Liz-Marzan, I. Lado-Tourino, *Langmuir*, **12**, 3585(1996), http://dx.doi.org/10.1021/la951501e
7. K. Esumi, T. Tano, K. Torigoe, K. Meguro, *Chemistry of Materials*, **2(5),** 564(1990), https://doi.org/10.1021/cm00011a019
8. M. P. Pileni, *Pure and Applied Chemistry*,**72**, 53(2000), https://doi.org/10.1351/pac200072010053

9. Y. P. Sun, P. Atorngitjawat, M. J. Meziani, *Langmuir*, **17**, 5707(2001), https://doi.org/10.1021/la0103057
10. J. Huang, Q. Li, D. Sun, Y. Lu, Y. Su, X. Yang, *Nanotechnology*, **18(10)**, 105104(2007), https://doi.org/10.1088/0957-4484/18/10/105104
11. V. Kumar, S. K. Yadav, *Journal of Chemical Technology and Biotechnology*, **84**, 151(2009), https://doi.org/10.1002/jctb.2023
12. G. Kalpana, R. B. Rishi, *Forest Ecology and Management*, **257**, 2066(2009)
13. H. Qamar, S. Rehman, D. K. Chauhan, *Current Drug Targets*, **20**, 1227(2019), http://dx.doi.org/10.2174/1389450120666190429120314
14. N. C. Shah, *Journal of Ethnopharmacology,* **6**, 293(1982), https://doi.org/10.1016/0378-8741(82)90052-6
15. A. K. Singh, A. S. Raghubanshi, J. S. Singh, *Journal of Ethnopharmacology,* **81**, 31(2002), https://doi.org/10.1016/S0378-8741(02)00028-4
16. M. Martínez-Cabanas, M. López-García, J.L. Barriada, R. Herrero, M.E. Sastre De Vicente, *Chemical Engineering Journal*, **301** 83(2016), https://doi.org/10.1016/j.cej.2016.04.149
17. S. Vasantharaj, N. Sripriya, M. Shanmugavel, E. Manikandan, A. Gnanamani, P. Senthilkumar, *Journal of Photochemistry and Photobiology B: Biology,* **179,** 119(2018), https://doi.org/10.1016/j.jphotobiol.2018.01.007
18. B. Kumar, K. Smita, L. A. Cumbal, Debut, *Journal of Saudi Chemical Society,* **18,** 364(2014), https://doi.org/10.1016/j.jscs.2014.01.003
19. F. Erci, R. Cakir-Koc, M. Yontem, E. Torlak, *Preparative Biochemistry & Biotechnology,* **50**, 538(2020), https://doi.org/10.1080/10826068.2019.1711393
20. P. Malik, R.K. Ameta, M. Singh, *Chemico-Biological Interactions,* **222,** 77(2014), https://doi.org/10.1016/j.cbi.2014.07.013
21. R.K. Ameta, M. Singh, *Journal of Molecular Liquids,* **195,** 40(2014), https://doi.org/10.1016/j.molliq.2014.01.029
22. R. K. Ameta, M. Singh, R. K. Kale, *New Journal of Chemistry,* **37,** 1501(2013), https://doi.org/10.1039/c3nj41141a
23. R.K. Ameta, R. Patel, P. Vijay, N. Sekhda, *Journal of Molecular Liquids*, **230,** 214(2017), https://doi.org/10.1016/j.molliq.2016.12.115
24. J. L. Elechiguerra, J. L. Burt, J. R. Morones, A.C. Bragado, X. Gao, H. L. Lara, M. J. Yacaman, *Journal of Nano Biotechnology*, **3**, 6(2005), https://doi.org/10.1186/1477-3155-3-6
25. E. C. Njagi, H. Huang, L. Stafford, H. Genuino, H. M. Galindo, J. B. Collins, G. E. Hoag, S. L. Suib, *Langmuir*, **27**, 264(2011), https://doi.org/10.1021/la103190n
26. I. Johnson, *Int J Mod Sci*, **1(4),** 237(2015), https://doi.org/10.1016/j.kijoms.2015.12.003
27. M. Sastry, M. Rao, and K. N. Ganesh, *Accounts of Chemical Res*earch, **35(10)**, 847(2002), https://doi.org/10.1021/ar010094x
28. J. Parmar, S. R. Sangani, M. Kawad, S. Korgaokar, M. Christy, M. Afzal, A. Alarifi, R. K. Ameta, *Journal of Molecular Structure*, **1288**, 135801(2023), https://doi.org/10.1016/j.molstruc.2023.135801

[RJC-9198/2024]